Macromolecular Chemistry and Physic
www.mcp-journal.d

Effect of Macromolecular Crowders on the Self-Assembly Process of Silk Fibroin

*Priyanka Dubey, Sinchan Seit, Pramit K. Chowdhury, and Sourabh Ghosh**

Macromolecular crowding is known to have a significant impact on the aggregation and folding of proteins. In this study, the role of different macromolecular crowders such as polyethylene glycol (PEG 200 and PEG 6000) and dextran (dextran 6000 and 70000) on the self-assembly of silk fibroin protein is explored. The data show that crowders induce a clear transition from random coil to β-sheet secondary conformation in the fibroin as demonstrated by ThT fluorescence spectroscopy, circular dichroism, and ATR-FTIR findings. However, this transition is not observed in case of control sample (fibroin without crowders). Excluded volume effects accelerate the kinetics of self-association of the fibroin protein. Increasing the molecular weight of crowders increases the required time for maximum aggregation. This study suggests that treating the fibroin with different macromolecular crowders has modulated the propensity of fibroin going into β-sheet conformation.

1. Introduction

Extensive efforts have been made to artificially spin native or regenerated silk fibroin protein or recombinant silk proteins by dry spinning,[1] wet spinning,[2] microfluidic spinning,[3] and by optimizing the post-spinning operations.[4] But even after hundreds of years of efforts, artificially spun silk fiber is still far from matching the properties of spun native silk fibers by the silkworm.[5]

Bombyx mori silk fiber is composed of two parallel filaments of fibroin protein, which are held together by the sericin protein. Sericins are hydrophilic glycoproteins that account for 25–30% of the total silkworm cocoon by weight. On the other hand, fibroin is a hydrophobic structural protein consists of a heavy chain of ≈390 kDa and light chains of ≈26 kDa linked by a single disulfide bond and the non-covalently attached 27–30 kDa polypeptide fibrohexamer.[6] So far most of the studies on self-assembly of regenerated silk protein and fiber spinning have focused solely on formation of the β-sheet crystalline structure of silk fibroin. Excellent tensile strength to the silk fiber results from its stable β-sheet structure as well as highly organized orientation of those crystalline domains.[7] Amphiphilic sequences in fibroin protein play a crucial role in the transition of secondary structures to the micellar folded structures,[8] which is governed by various factors, such as pH,[9] metallic ions, and shear. Among all these determinants, shear stress is thought to be most critical for transition of silk fibroin chains from a random coil conformation to a β-sheet structure in aqueous solution.[10] However, dissolution and reconstitution processes of fibroin protein significantly disrupt the native hierarchical structure,[11] which cause significant difference between self-assembly mechanisms of fibroin proteins in silkworms' gland and in laboratory.

The role of sericin in modulating the self-assembly of fibroin within the gland of silkworm or during spinning is not very clear. One of the main reasons for this could be the difficulty in extracting sericin protein from silk fibers due to protein degradation during degumming.[12] Isolation of pure native sericin protein from silkworm gland is also a major challenge. As many as seven different types of sericin proteins are secreted within the gland at different regions, with molecular weight varying from 24 to 400 kDa.[13] A recent study has demonstrated that increasing the concentration of sericin helped in maintaining the silk I conformation by increasing the required time to form the β-sheet crystals.[14] Another study reported the presence of sericin could decrease crystallization and the mechanical property of the regenerated silk fibroin.[15] When the fibroin protein was blended with a hydrophilic polymer, such as hyaluronic acid, β-sheet crystallization was induced, even without methanol treatment or shear force.[16] Crystallinity and tensile strength of the regenerated silk filament, fabricated from partially degummed cocoons were higher than completely degummed regenerated silk.[17] These reports indicate that sericin seems to play an imperative role in the structure and mechanical property of fibroin by affecting the conformational transition of fibroin molecules. Also, sericin does not solidify within the gland or spinneret but gradually forms gel. This indicates that sericin may act as a macromolecular crowder and modulate the secondary conformations and self-assembly of fibroin,

P. Dubey, S. Seit, Prof. S. Ghosh
Department of Textile and Fibre Engineering
Indian Institute of Technology Delhi
Hauz Khas, New Delhi 110016, India
E-mail: Sourabh.Ghosh@textile.iitd.ac.in
Prof. P. K. Chowdhury
Department of Chemistry
Indian Institute of Technology Delhi
Hauz Khas, New Delhi 110016, India
The ORCID identification number(s) for the author(s) of this article can be found under https://doi.org/10.1002/macp.202000113.

DOI: 10.1002/macp.202000113

other than its lubricating interaction with fibroin inside the silk gland.

Macromolecular crowding is a well-known phenomenon in cellular biochemistry as the biological macromolecules collectively populate 10–40% of the fluid volume inside the cell cytoplasm.[18,19] This volume fraction restricts the volume available to other macromolecules of the cytoplasm.[20] Hence, crowded microenvironment alters the biological processes including protein folding and aggregation, protein self-assembly, and conformational transitions[18,21] as compared to those biological processes of proteins in dilute solutions, primarily due to the phenomenon referred to as the "excluded volume effect."

Taken together, it would be interesting to determine the effect of macromolecular crowders, as an approximate mimic of the protein sericin, on the self-assembly process of silk fibroin. A study has shown that addition of polyethylene glycol (PEG 600) in regenerated fibroin solution did induce a more rapid and triggered gelation.[22] However, another study stated that PEG 600 hindered the structural transition of fibroin solution from random coil or α-helix to β-sheet conformation.[23] Dextran is another highly water soluble crowder used to modulate folding characteristics of some proteins.[24,25] However, its effect on silk fibroin self-assembly is still unknown. Thus it would be interesting to determine the effect of these commonly used macromolecular crowders on the self-assembly process of silk fibroin and the underlying mechanism in the structural transition.

The polymorphic (random coil, silk I, II, and III) behavior of silk fibroin opens up a window to modulate its structural transitions during self-assembly for different functional outcomes. Depending on various factors such as coagulants (e.g., alcohol), temperature, different processing conditions, etc., fibroin protein may form a fibrillar structure akin to amyloid.[26,27] A study illustrated the occurrence of amyloids in the spleens of five out of seven mice after injecting the regenerated silk fibrils to mice,[28] which putatively might occur due to silk fibroin self-assembly under the effect of macromolecular crowders in mouse spleen. Thus, it would be interesting to determine whether presence of these macromolecular crowders can induce β-sheet crystallization in silk fibroin resembling amyloids-like cross β-sheet crystals or parallel β-sheet crystals.

2. Results

2.1. Turbidity Analysis of Fibroin Incubated with Different Crowders

The turbidity analysis of fibroin as a function of the concentration of the different crowders showed distinct fibrillation kinetics. Fibroin in the presence of 50, 100, and 150 mg mL^{-1} of PEG 200 had the LOGt_0 (time in hours required for half maximum response) at 11.71, 7.29, and 4.63 h, respectively, since incubation for aggregation (**Figure 1**a). In presence of PEG 6000, the silk protein showed LOGt_0 values of 19.27, 10.10, and 6.6 h for 50, 100, and 150 mg mL^{-1} concentrations of PEG 6000, respectively (Figure 1b). These data thus show that increasing the concentration of PEG 200 and 6000 accelerated the aggregation of fibroin (**Table 1**). Similar experiments were also conducted with the different dextran based crowders, i.e., dextran 6000 and 70 000. Fibroin incubated with dextran 6000 showed that increasing the crowder concentration (50, 100, and 150 mg mL^{-1}) decreases the time required for maximum aggregation as observed from the decrease in LOGt_0 values (17.5, 14.61, and 8.71 h, respectively) (Figure 1c).

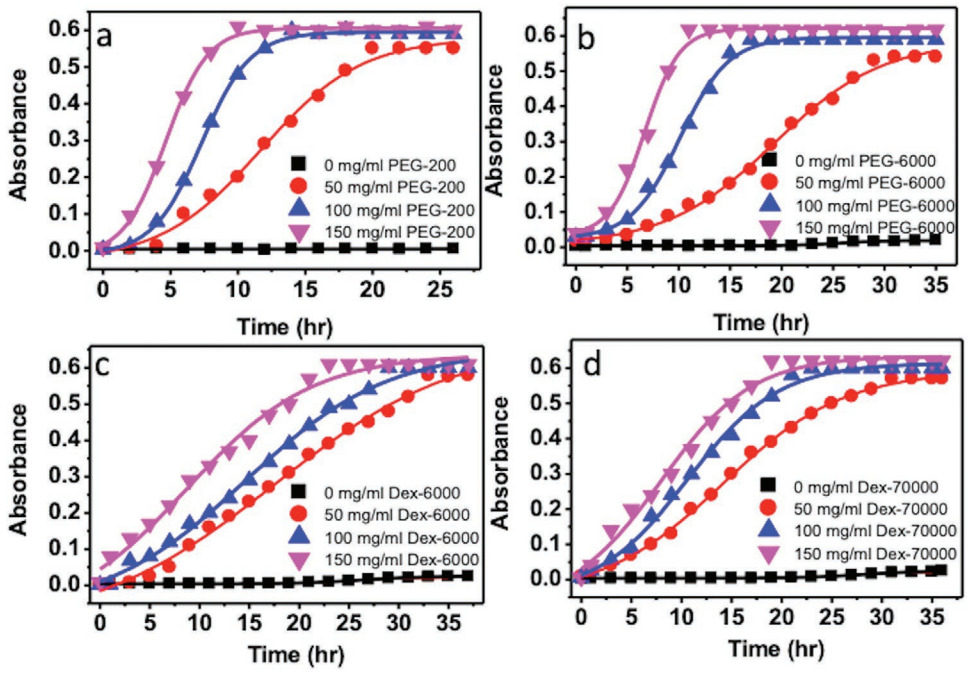

Figure 1. Turbidity analysis of fibroin solution (10 mg mL^{-1}) incubated with different concentrations (50, 100, and 150 mg mL^{-1}) of a) PEG 200, b) PEG 6000, c) dextran 6000, and d) dextran 70 000. Absorbance was recorded at 600 nm at regular interval of 2 h.

Table 1. Turbidity and ThT fluorescence of fibroin incubated with different crowders. LOGt_0 represents the time (hours) required for half maximum response.

S. No.	Sample names and concentrations	Turbidity analysis (LOGt_0)	ThT fluorescence (LOGt_0)
i	Fibroin with PEG 200		
	a) 50 mg mL^{-1}	11.71	10.60
	b) 100 mg mL^{-1}	7.29	6.80
	c) 150 mg mL^{-1}	4.63	3.48
ii	Fibroin with PEG 6000		
	d) 50 mg mL^{-1}	19.27	18.48
	e) 100 mg mL^{-1}	10.10	9.93
	f) 150 mg mL^{-1}	6.6	5.6
iii	Fibroin with dextran 6000		
	g) 50 mg mL^{-1}	17.5	16.9
	h) 100 mg mL^{-1}	14.61	13.02
	i) 150 mg mL^{-1}	8.71	7.09
iv	Fibroin with dextran 70 000		
	j) 50 mg mL^{-1}	14.11	13.57
	k) 100 mg mL^{-1}	10.57	9.49
	l) 150 mg mL^{-1}	7.93	6.03

Similarly, fibroin incubated with dextran 70 000 at concentrations of 50, 100, and 150 mg mL^{-1} showed half maxima (LOGt_0) at 14.11, 10.57, and 7.93 h (Figure 1d), which is less than fibroin incubated with dextran 6000. Thus, increasing the crowder concentration enhanced the rate of aggregation of fibroin.

2.2. Aggregation Kinetics of Fibroin with Crowders Using ThT Fluorescence

In order to confirm the self-association kinetics obtained using turbidity analysis, ThT fluorescence assay was carried out. ThT data showed that fibroin incubated with PEG 200 crowder showed the LOGt_0 (time required for half maximum response) at 10.60, 6.80, and 3.48 h, for 50, 100, and 150 mg mL^{-1}, respective concentration of crowders (**Figure 2**a). However, with PEG 6000 the LOGt_0 values were increased to 18.48, 9.93, and 5.6 h, respectively for 50, 100, and 150 mg mL^{-1} concentration, thereby showing a similar qualitative trend as the turbidity analysis (Figure 2b). Fibroin incubated with 50, 100, and 150 mg mL^{-1} concentration of dextran 6000 showed the half maximum aggregation kinetics LOGt_0 at 16.90, 13.02, and 7.09 h, respectively (Figure 2c), whereas dextran 70 000 showed LOGt_0 at 13.57, 9.49, and 6.03 h for 50, 100, and 150 mg mL^{-1} concentration respectively (Figure 2d). Therefore the trend obtained from the ThT data was qualitatively similar to that obtained by the turbidity analysis.

2.3. Secondary Structure Analysis by CD Spectroscopy

Fibroin incubated with all four crowders, PEG (200, 6000) and dextran (6000, 70 000) at 0 min (initial time point) demonstrated

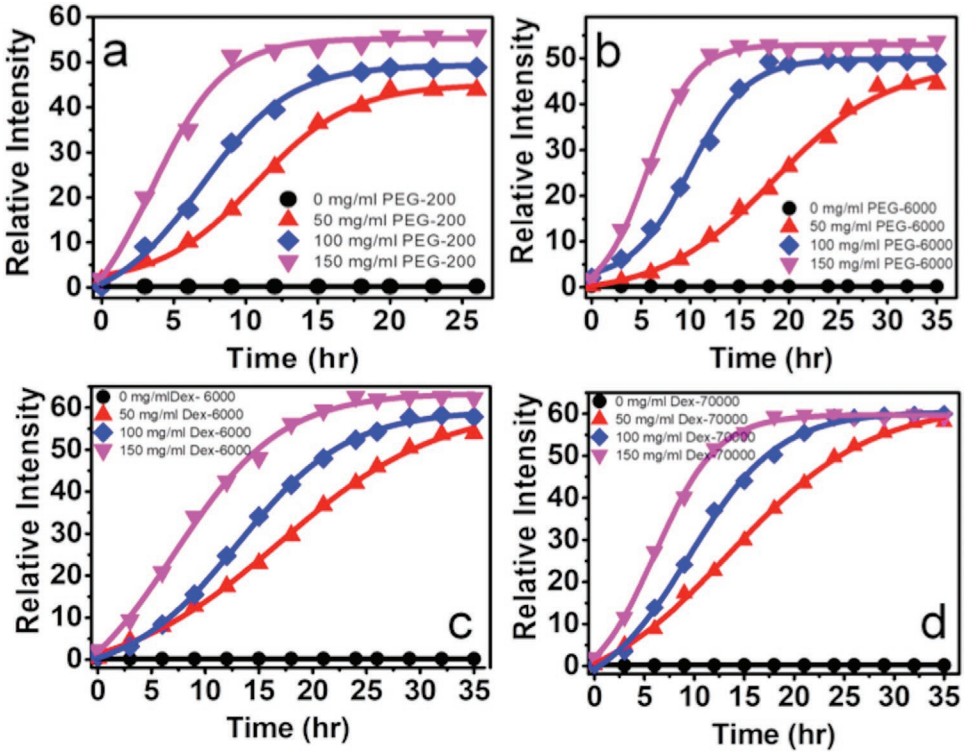

Figure 2. Aggregation kinetics of fibroin measured by thioflavin T fluorescence. Aggregation kinetics of fibroin incubated with a) PEG 200, b) PEG 6000, c) dextran 6000, and d) dextran 70 000. All spectra were recorded at three different concentration of crowders (50, 100, and 150 mg mL^{-1}) along with control (fibroin without crowder, i.e., 0 mg mL^{-1}) at 25 °C.

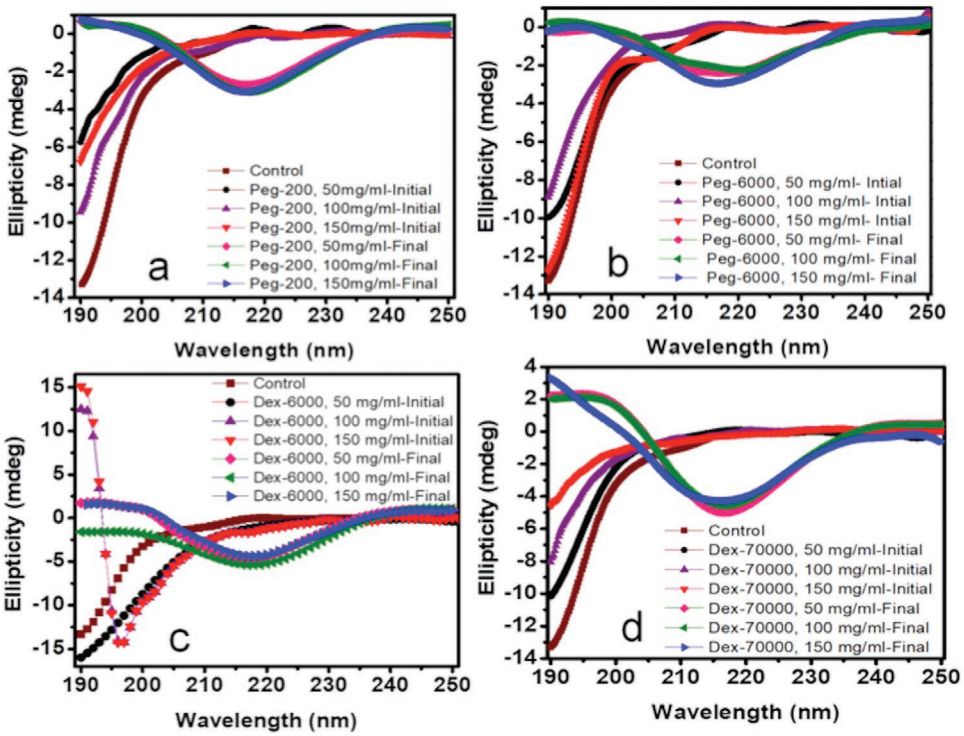

Figure 3. CD spectroscopy of fibroin incubated with different concentrations of the crowders at initial and final time points. CD spectra of fibroin (10 mg mL^{-1}) incubated with a) PEG 200, b) PEG 6000, c) dextran 6000, and d) dextran 70 000.

a peak of random coil conformation similar to the control, fibroin without crowder, at 0 min (**Figure 3**). However, prolonged incubation of fibroin with 50, 100, and 150 mg mL^{-1} concentration of PEG 200 showed a transition from random coil to β-sheet conformation at 20, 14, and 7 h, respectively (Figure 3a), similar to the ThT saturation time points (Figure 2). A similar observation was made with the 50, 100, and 150 mg mL^{-1} PEG 6000, wherein transition was observed at 35, 20, and 11 h respectively (Figure 3b). However, this transition was not observed in case of control (fibroin without PEG) at the same time points wherein fibroin retained its random coil conformation.

Fibroin incubated with dextran 6000 and 70 000 (50, 100, 150 mg mL^{-1} concentration) followed the similar trend as observed in presence of PEG. All samples with and without crowders showed a random coil conformation at 0 min however, with further incubation it results into transition from random coil to β-sheet conformation except excluding control (fibroin without crowder). The 50, 100, and 150 mg mL^{-1} concentrations of dextran 6000 lead to the β-sheet transition at 33, 27, and 15 h (Figure 3c), whereas dextran 70 000 (50, 100, and 150 mg mL^{-1}) showed β-sheet conformation at 28, 20, and 13 h respectively as illustrated in Figure 3d. Thus the CD data, in accordance with the turbidity analysis and ThT studies, confirmed the presence of fibroin aggregates having β-sheet structure.

2.4. ATIR-FTIR Spectroscopy of Fibroin with Crowders

ATR-FTIR spectroscopy of fibroin was carried out in order to probe the secondary structural composition of fibroin in the presence of different crowders by monitoring changes in the amide I region as illustrated in **Table 2**. As shown in **Figure 4**a,

Table 2. ATR-FTIR deconvolution data of (i) fibroin with PEG 200, (ii) fibroin with PEG 6000, (iii) fibroin with dextran 6000, and (iv) fibroin with dextran 70 000 recorded in the amide I region (1600–1700 cm^{-1}).

S. No.	Concentrations	Initial time point		Final time point	
		Random coil [%]	β-Sheet	Random coil [%]	β-Sheet
i	Fibroin with PEG 200				
	a) 50 mg mL^{-1}	53	0	0	57
	b) 100 mg mL^{-1}	50	0	0	61
	c) 150 mg mL^{-1}	55	0	0	58
ii	Fibroin with PEG 6000				
	a) 50 mg mL^{-1}	60	0	0	48
	b) 100 mg mL^{-1}	53	0	0	55
	c) 150 mg mL^{-1}	50	0	0	47
iii	Fibroin with dextran 6000				
	a) 50 mg mL^{-1}	52	0	0	57
	b) 100 mg mL^{-1}	54	0	0	53
	c) 150 mg mL^{-1}	61	0	0	62
iv	Fibroin with dextran 70 000				
	a) 50 mg mL^{-1}	53	0	0	56
	b) 100 mg mL^{-1}	54	0	0	57
	c) 150 mg mL^{-1}	53	0	0	57

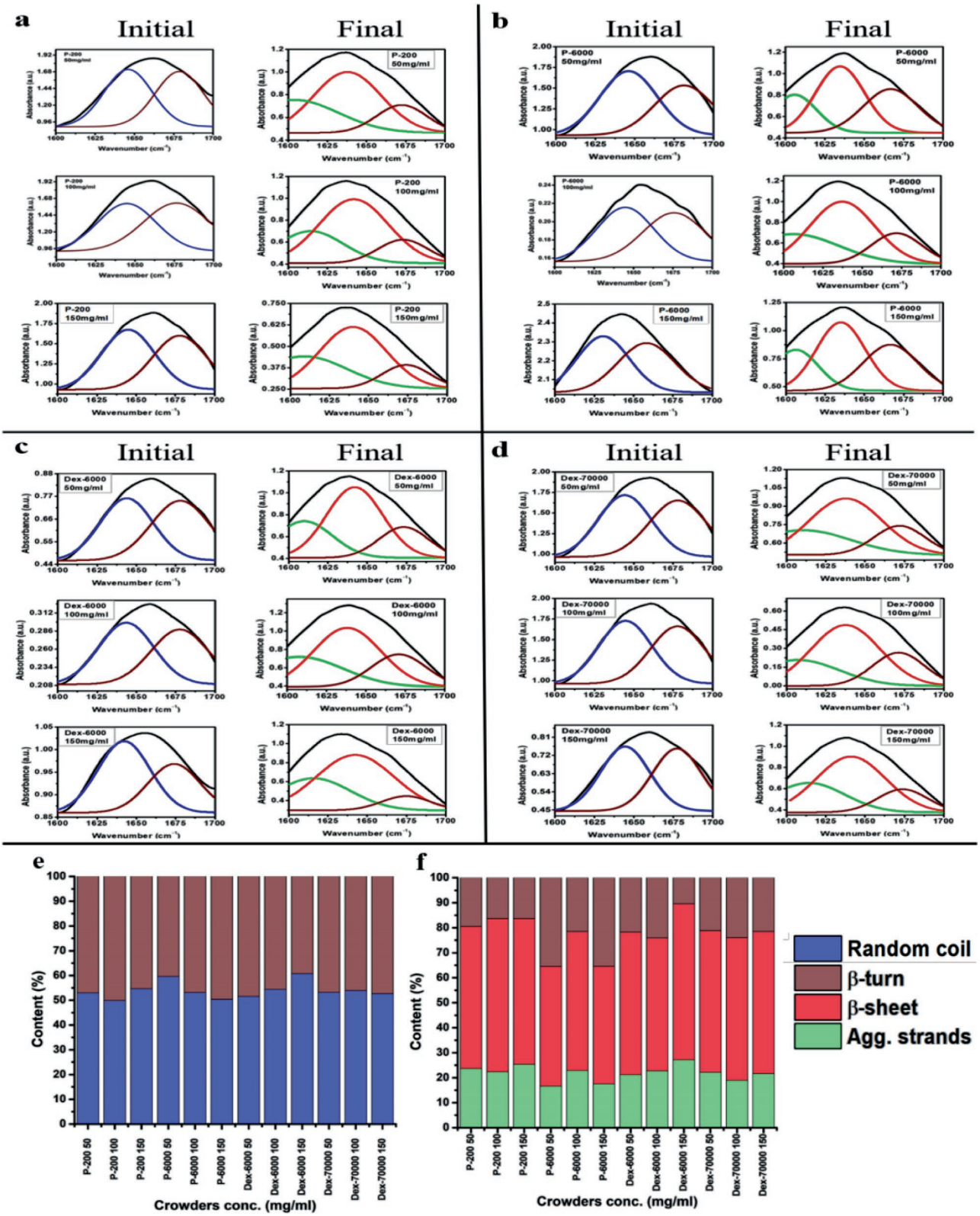

Figure 4. ATR-FTIR of fibroin incubated with different concentrations of a) PEG 200, b) PEG 6000, c) dextran 6000, and d) dextran 70 000. ATR-FTIR of fibroin with 50, 100, and 150 mg mL^{-1} concentrations of PEG-200 and PEG 6000 at their initial (0 min) and their subsequent final time points were conducted. e,f) The total initial and final secondary structural components of all the samples. The different colors of spectra are representing different secondary conformations such as: random coil (blue), β-turn (brown), β-sheet (red), and aggregated strands (green).

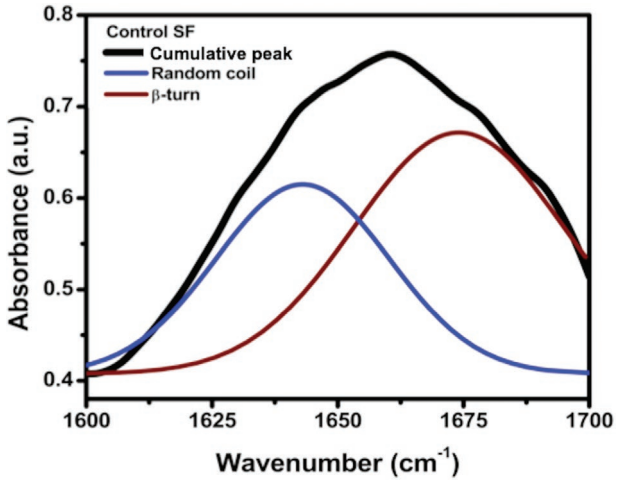

Figure 5. ATR-FTIR spectra of fibroin without crowders recorded at 36 h, which is a maximum aggregation time of fibroin in the presence of crowders.

the dominant random coil conformation of fibroin with different concentrations (50, 100, and 150 mg mL^{-1}) of PEG 200 at the initial time point showed the random coil conformation, which is replaced by β-sheet at the final time point. However, this transition was not observed in case of control (i.e., fibroin without crowders, **Figure 5**).

Similar observation was made when fibroin was incubated with PEG 6000. The representative IR spectra of fibroin at 50, 100, and 150 mg mL^{-1} concentrations of PEG 6000 (initial and final time points) are shown in Figure 4b. The predominant random coil peaks at the initial time points (50, 150 mg mL^{-1} PEG 6000 concentrations) are replaced by peaks around 1635–1639 cm^{-1} at the final time points indicating formation of β-sheet structure.[29] Similar results were obtained when fibroin was incubated with dextran 6000 and 70 000. As shown in the representative FTIR spectra of fibroin (Figure 4c,d), the dominant random coil conformational peaks of dextran 6000 and 70 000 at the initial time points were replaced by β-sheet structure in the final time points.

Taken together the data revealed that the different concentrations (50, 100, and 150 mg mL^{-1}) of different crowders (PEG 200, PEG 6000, dextran 6000, and dextran 70 000) showed a transition from random coil and β-turns (at initial time points) to β-sheet and aggregate strands at their final time points along with a significant decrease in the β-turn conformation. However, in case of fibroin incubated without crowder (control) till 36 h, which was considered as a maximum aggregation time required to achieve the saturation showed the presence of random coil without the formation of β-sheet (Figure 5). Therefore, it can be deduced that the presence of crowders has a significant impact on the structural transition of silk fibroin as validated by CD finding as well.

2.5. AFM of Fibroin Incubated with Different Crowders

Atomic force microscopy experiments were further performed to monitor the effect of the macromolecular crowding agents on the morphology of the silk protein fibrils. The AFM image of fibroin incubated with PEG 200 at 0 min showed a 0.39, 1.59, and 1.66 nm of roughness at 50, 100, and 150 mg mL^{-1} concentration of crowder. However, with prolonged incubation at their respective final time points roughness increased to 13.3, 20.2, and 26.7 nm as showed in Figure S2(i) (Supporting Information). However, the AFM study of fibroin without addition of crowder (control) has showed the roughness of 1.3 and 1.24 nm at initial (0 min) and final time point (36 h) respectively (Figure S1, Supporting Information). Similarly, fibroin incubated with PEG 6000 showed 0.546, 2.37, and 2.82 nm roughness at 0 min, initial time point (Figure S2(ii), Supporting Information). However, at their respective final time points, all the samples of fibroin with PEG 6000 showed increased roughness at all three concentrations (50, 100, and 150 mg mL^{-1}) to 17, 18.9, and 20.2 nm as demonstrated in Figure S2(ii) (Supporting Information).

AFM images of fibroin incubated with dextran 6000 at 0 min (initial time point) demonstrated a roughness value of 1.75, 3.5, and 0.82 nm at 50, 100, and 150 mg mL^{-1} concentrations of fibroin with dextran 6000 crowder respectively (Figure S3(i), Supporting Information). However, at their respective, final time points roughness increased to 13.9, 23.9, and 22.8 nm (Figure S3(i), Supporting Information). A similar trend was observed when fibroin was incubated with dextran 70 000 where roughness was increased in each sample from initial 0 min (Figure S3(ii), Supporting Information) to final time points (Figure S3(ii), Supporting Information). Fibroin with 50, 100, and 150 mg mL^{-1} concentration of crowder (dextran 70 000) showed an increased roughness from 1.69 to 20.5, 1.86 to 12.3, and 1.67 to 20.41 nm (from initial to respective final time point).

3. Discussion

B. mori silk fibroin fiber is comprised of two proteins, namely 20–30% sericin and 70–80% fibroin. Sericin can be classified as sericin A, B, and C based on its solubility and origin of secretion in the gland. Sericin A and B consist of serine, threonine, glycine, aspartic acid as the predominant amino acids whereas sericin C has proline additionally.[30] However, it is not feasible to throw light onto the interactions between sericin and fibroin during coacervation and self-assembly process of silk fibroin, as sericins get denatured during degumming. Identification of synthetic crowding agents having defined chemical composition and molecular weight would help in induction of precisely controlled silk fibroin self-assembly. Therefore, the current study explored the role of different macromolecular crowders (PEG and dextran) on the self-assembly process of silk fibroin.

During aggregation of proteins or protein fragments, spontaneous conformational conversion (misfolding) may result in the development of a cross β-sheet fold, amyloids, which lead to various pathological conditions.[31] Amyloid formation is commonly studied in vitro in dilute conditions in presence of buffer solutions, but such experimental conditions fail to recapitulate the in vivo intracellular environment crowded by various macromolecules. In vitro, macromolecular crowded environment is commonly replicated by adding various crowding agents, such as hydrophilic and neutral polysaccharides (e.g., Ficoll or dextran).[24,32] Studies on various amyloidogenic proteins

(prion protein, apolipoprotein C-II, Aβ, α-synuclein, hyperphosphorylated Tau 244–441, etc.) demonstrated that these crowding agents (Ficoll or dextran) enhanced amyloidogenesis, as the rate of encounter of amyloid precursors get enhanced due to the volume exclusion effect.[33,34] The cross β-sheet signatures can be traced out from the infrared spectral peaks between 1611 and 1630 cm^{-1} range with partially overlapping native β-sheet peak region from 1630 to 1643 cm^{-1}.[35]

In the current study, dextran and PEG were used as macromolecular crowders for modulating the silk fibroin self-assembly process. Dextran is widely accepted as a near-perfect model for a macromolecular crowder since its interaction with proteins can be described using pure excluded-volume models.[36] On the other hand, PEG is a crowding agent whose interactions with proteins cannot be described quantitatively in terms of excluded volume alone.[37] PEG has been reported to affect the conformational and aggregation behavior of various structurally different proteins, ranging from natively unfolded (e.g., core histones and α-synuclein) to folded proteins (e.g., insulin).[38] Hence, we hypothesized that the transition from random coil to β-sheet conformation in silk fibroin will be favored in their presence.

Our data showed that both types of crowders (dextran and PEG based) induce a clear transition from random coil to β-sheet conformation, including aggregated β-sheet structure. However, this transition was not observed in case of control (fibroin without crowder), as demonstrated by CD, ATR-FTIR, and ThT fluorescence measurements. It was also observed that increasing the concentration of crowders decreased the time required for aggregation.

The effect of macromolecular crowders on protein aggregation can be varied in nature.[39] In some cases the excluded volume effect exerted by the crowding agents increases the local concentration of the aggregating protein units, leading to increase in collision frequency and hence enhancing aggregation kinetics.[40] On the other hand, aggregation may decrease in presence of the crowders due to native state stabilization of the protein under investigation.[41] Keeping in mind the fact that increase in the concentration of the crowding agents also results in an increase in the viscosity of the solution, our data suggest that indeed the excluded volume plays a major role wherein self-association of the fibroin protein units is accelerated. This is further confirmed by the fact that no observable gain in secondary structure is obtained (Figure 3) for the disordered silk fibroin as a function of the crowding agents, suggesting negligible stabilization of protein structure in presence of the crowders.

Increased amount of crowding agent would elevate the excluded volume. This would in turn lead to an enhancement of the kinetics of aggregation. Interestingly, fibroin with higher molecular weight crowder (PEG-6000) showed that increasing the molecular weight also increases the required time for maximum aggregation as compared to PEG 200. The difference observed between the effects of these two crowders on fibroin may be attributed to the extent of the volume excluded by the crowders belonging to the same family but having different molecular weights. For the low molecular weight crowder, at a given concentration (in g L^{-1}), the density is higher as compared to that of high molar mass. Based on this scenario, the low molecular weight crowder, here, PEG 200 exerts an appreciably higher excluded volume, the same being reflected in the differences in the aggregation rates. However, this aspect cannot be generalized as is understood while comparing among the dextran based crowding agents, wherein dextran 70 000 shows a higher rate in aggregation than dextran 6000, in spite of the latter exhibiting a higher number density. Indeed, predicting the effect of such crowders is not easy as also been shown wherein multiple factors come into play including the nature (i.e., open chain as in PEG or rigid systems as for the dextrans) and shape of the polymer.[42] Shape of the crowder is one of the crucial factors accountable for diminution of the translational diffusion coefficient and have a direct influence on the aggregation of proteins.[43] Another study demonstrated the importance of flexibility (i.e., the changing transient shape) in the crowding system, however they also stated that charge does not play an important role in the macromolecular crowding.[44] Zegarra et al.[45] showed that unfolded protein, apoazurin turns elongated in the presence of dextran. They revealed that rod-like shape of the dextran stabilizes an elongated conformation and facilitate an anisotropic direction of the depletion force between the protein and crowders. Another study has showed that stability of proteins may directly influence by the size and shape of the crowders.[46] They observed that by increasing the crowder concentration, the extent of stability has also been increased due to presence of small-sized and rod-shaped (dextran 40) crowder. Increasing the complexity of crowder–protein interactions is the fact that macromolecular crowding agents have also been shown to exhibit soft interactions with the protein thereby further affecting the aggregation landscape. Thus, the observed effect of the crowders on the aggregation of silk fibroin is a combination of all these aforementioned effects.

In a recent paper, Lemetti et al.[47] studied the self-assembly of a 84 kDa triblock recombinant protein, which is relevant to spidroin silk, in presence of crowding agents. Crowding agents reduced the protein concentration at which coacervation takes place. Fibroin predominantly contains repetitive hexapeptide GAGAGS sequences, as well as GAGAGY and GAGAGVGY sequences, which imparts hydrophobicity.[48,49] During gelation and self-assembly of fibroin protein, the above mentioned sequences play a critical role in the secondary structure transitions leading to the formation of anti-parallel β-sheet structure.[50,51] Interestingly, silk biomaterials occasionally have been shown to cause amyloidogenic depositions based on the presence of above mentioned secondary conformations, processing conditions.[27] Injection of regenerated silk fibrils to mice caused deposition of mild to moderate extent of amyloids in spleens of five out of seven mice.[28] These studies show that although fibroin fibrils are non-pathogenic β-sheet rich protein and show reduced the initial lag phase during self-assembly in aqueous medium, but in vivo they may lead to amyloidogenesis, based on chronic inflammatory microenvironment or presence of biological macromolecules.[28] This is of significant clinical interest, as silk fibers are dissolved and scaffolds for tissue engineering strategies are developed using reconstituted silk fibroin protein, it may lead to amyloidogenesis at the site of the injury in inflammatory milieu. Our findings highlighted the absence of amyloidogenic cross β-sheet conformation in presence of crowders. This indicates that probably the native β-sheet containing proteins such as fibroin requires an

appreciable structure reorganization during conformational change to form cross β-sheet (amyloid) conformation, which would not happen in static condition.

Thus, the importance of the current study stems from the observation that the crowders, depending on their nature, have the potential of bringing about alterations of the fibroin conformation and kinetics of self-association. Thus, our current study demonstrates that PEG or dextran at suitable concentrations may serve as effective macromolecular crowders in conversion of the random coil structure of the fibroin protein to a predominantly stable β-sheet structure. A recent study[52] used microfluidics setup with ion gradients in coaxial flow thereby improving the mechanical sheering of silk. However, extensional flow alone is not sufficient to create fibers at natural spinning speeds and physiological changes such as significant change in pH and high metal ion concentrations are required in order to improve the spinnability of silk.[52] Therefore, future step would be to use macromolecular crowding agents combined with microfluidics setup for in vitro mimicking of the natural self-assembly of silk fibroin to spin artificial silk filament. Next logical step will be to use the mixed crowding scenario by using binary and ternary crowder systems.

4. Conclusion

Both the crowders (dextran and PEG) modulated the self-assembly of silk fibroin and induced a clear transition from random coil to β-sheet conformation. Increasing the concentration of crowders resulted in lesser time needed for aggregation. The thioflavin T binding was evident in fibroin incubated with PEG or dextran, but AFM data did not show the presence of fibrillar structures, typical of amyloid nature of aggregation. We could not find existence of amyloidal cross β-sheet structure in crowded microenvironment.

5. Experimental Section

Materials: Polyethylene glycol (MW 200 and 6000), lithium bromide (LiBr), and sodium carbonate (Na_2CO_3) were purchased from Merck (India). Dextran (MW 6000 and 70 000) was procured from Himedia (India). Thioflavin T (purity >97%) was purchased from Sigma-Aldrich (USA). *B. mori* cocoons were procured from Central Silk Technological Research Institute (Central Silk Board), Bangalore, Ministry of Textiles, Government of India. All the other used chemicals were of analytical grade.

Regenerated Aqueous Solution Preparation of Silk Fibroin from Cocoons: Regenerated aqueous fibroin solution from *B. mori* cocoons was prepared as mentioned previously.[31] Degumming of cocoons was carried out using 0.02 M Na_2CO_3 in boiling water in order to remove the sericin protein. Degummed silk fibers were thoroughly washed by ultrapure deionized water (resistivity ≈18.2 MΩ cm) followed by drying at 50 °C in an oven. Washed and dried fibroin fibers were further dissolved in 9.3 M LiBr at 60 °C for 4 h. The obtained solution after dissolution was further dialyzed against the ultrapure deionized water for 48 h to remove the LiBr salt.

Preparation of PEG (MW 200, 6000) and Dextran (MW 6000, 70 000) Solution: The stock solution of 400 mg mL^{-1} concentration of PEG (200, 6000) and dextran (6000, 70 000) was prepared and diluted further in milli-Q to acquire the final concentration of 50, 100, and 150 mg mL^{-1}.

Self-Assembly of Silk Fibroin with Different Crowders at 600 nm: The stock of 50 mg mL^{-1} fibroin solution was diluted with milli-Q water to prepare the final 10 mg mL^{-1} concentration. Fibroin solution was incubated with 50, 100, and 150 mg mL^{-1} concentrations of both PEG (MW 200, 6000) for 26 and 36 h, respectively. Similar concentrations (50, 100, and 150 mg mL^{-1}) were used with dextran (MW 6000, 70 000) for 36 h. Samples were incubated at 25 °C and aliquots were collected at regular intervals. Fibroin incubated without crowder was used as control. The self-assembly kinetics of fibroin with and without crowders were analyzed by UV–vis spectrophotometer (UV-2450, SHIMADZU, Japan) at 600 nm.

ThT Fluorescence Spectroscopy: The ThT fluorescence emission spectra of fibroin with or without crowders were recorded in the range of 440–700 nm with excitation at 430 nm at 25 °C using Edinburg Spectrofluorimeter (FLS920, Edinburgh Instruments, UK). The excitation and emission slit widths were kept at 2 and 5 nm, respectively. The stock solution of 1×10^{-3} M concentration was diluted to obtain the final 20×10^{-6} M concentration of ThT and was filtered through 0.22 µm filter. All spectra were recorded thrice using a 10 mm path length quartz cuvette and were normalized for milli-Q water contribution. Furthermore, sigmoidal curve data fitting was carried out with OriginPro 8.5 (Origin Lab Corporation, Northampton, MA, USA) using following equation:

$$Y = A1 + \frac{A2 - A1}{1 + 10^{\mathrm{LOG}t_0 - tp}} \quad (1)$$

where Y is intensity of ThT fluorescence, $A2$ and $A1$ are the Y values at the top and the bottom of the curve, respectively. $\mathrm{LOG}t_0$ is the time (in hours) required for half maximum response. The Hill slope or Hill coefficient is represented by p.[53,54]

Circular Dichroism Measurements: CD spectroscopy was carried out in the far-ultraviolet (UV) range of 190–260 nm at 25 °C using 1 mm path length quartz cuvette in Jasco J-815 CD spectrometer (Jasco Corporation, Tokyo, Japan). Spectra were recorded in a 0.01 cm cell with a bandwidth of 1.0 nm. All spectra were normalized for milli-Q water contribution.[8]

Attenuated Total Reflectance-Fourier Transform Infrared Spectroscopy: ATR-FTIR was carried out in the absorption mode using Perkin-Elmer (Spectrum BX Series, MA, USA) instrument. All spectra were recorded in the 1700–1600 cm^{-1} amide I region with DTGS (Deuterated Triglycine Sulfate) IR detector. 64 scans per sample were recorded at a resolution of 4 cm^{-1} and was further deconvoluted using OriginPro 8.5 (Origin Lab Corporation, Northampton, MA, USA).[55] Baseline correction and area normalization were carried out prior to deconvolution.

Atomic Force Microscope Images: AFM (Dimension ICON with ScanAsyst, Bruker) of fibroin with and without crowders was performed in tapping mode with silicon probe (Tap 300 Al-G, Budget Probes, Sofia, Bulgaria). 10 µL of each sample was mounted on freshly cleaved mica, washed with milli-Q, and air dried further for ≈1 h. The NanoScope Software (Version 4.1) was used to analyze the roughness of all the samples.

Supporting Information

Supporting Information is available from the Wiley Online Library or from the author.

Conflict of Interest

The authors declare no conflict of interest.

Keywords

dextran, macromolecular crowding, PEG, self-assembly, silk fibroin

Received: March 30, 2020
Revised: June 28, 2020
Published online:

[1] W. Wei, Y. Zhang, Y. Zhao, J. Luo, H. Shao, X. Hu, *Mater. Sci. Eng., C* **2011**, *31*, 1602.
[2] J. Yan, G. Zhou, D. P. Knight, Z. Shao, X. Chen, *Biomacromolecules* **2010**, *11*, 1.
[3] Q. Peng, H. Shao, X. Hu, Y. Zhang, *Macromol. Mater. Eng.* **2017**, *302*, 1700102.
[4] K. Yazawa, A. D. Malay, N. Ifuku, T. Ishii, H. Masunaga, T. Hikima, K. Numata, *Biomacromolecules* **2018**, *19*, 2227.
[5] Y. Liu, J. Ren, S. Ling, *Comput. Commun.* **2019**, *13*, 85.
[6] S. Inoue, K. Tanaka, F. Arisaka, S. Kimura, K. Ohtomo, S. Mizuno, *J. Biol. Chem.* **2000**, *275*, 40517.
[7] D. N. Rockwood, R. C. Preda, T. Yucel, X. Q. Wang, M. L. Lovett, D. L. Kaplan, *Nat. Protoc.* **2011**, *6*, 1612.
[8] P. Dubey, S. Murab, S. Karmakar, P. K. Chowdhury, S. Ghosh, *Biomacromolecules* **2015**, *16*, 3936.
[9] P. R. Laity, C. Holland, *Int. J. Mol. Sci. 17*, **2016**, 1812.
[10] Y. Jin, Y. C. Hang, Q. F. Peng, Y. P. Zhang, H. L. Shao, X. C. Hu, *RSC Adv.* **2015**, *5*, 62936.
[11] S. R. Koebley, D. Thorpe, P. Pang, P. Chrisochoides, I. Greving, F. Vollrath, H. C. Schniepp, *Biomacromolecules* **2015**, *16*, 2796.
[12] D. Gupta, A. Agrawal, A. Rangi, *Indian J. Fibre Text. Res.* **2014**, *39*, 364.
[13] T. Gamo, *Biochem. Genet.* **1982**, *20*, 165.
[14] H. W. Kwak, J. E. Ju, M. Shin, C. Holland, K. H. Lee, *Biomacromolecules* **2017**, *18*, 2343.
[15] K. H. Lee, *Macromol. Rapid Commun.* **2004**, *25*, 1792.
[16] M. Garcia-Fuentes, E. Giger, L. Meinel, H. P. Merkle, *Biomaterials* **2008**, *29*, 633.
[17] C. S. Ki, J. W. Kim, H. J. Oh, K. H. Lee, Y. H. Park, *Int. J. Biol. Macromol.* **2007**, *41*, 346.
[18] A. C. Miklos, M. Sarkar, Y. Wang, G. J. Pielak, *J. Am. Chem. Soc.* **2011**, *133*, 7116.
[19] H. X. Zhou, *FEBS Lett.* **2013**, *587*, 1053.
[20] R. J. Ellis, *Trends Biochem. Sci.* **2001**, *26*, 597.
[21] R. J. Ellis, A. P. Minton, *Nature* **2003**, *425*, 27.
[22] H. J. Zhao, S. Y. Xiong, M. Z. Li, Q. Zhang, G. Y. Liu, *Adv. Mater. Sci. Eng.* **2012**, *2012*, 819464.
[23] S. Y. Xiong, Y. D. Cheng, Y. Liu, S. Q. Yan, Q. Zhang, M. Z. Li, *J. Fiber Bioeng. Inf.* **2011**, *3*, 236.
[24] A. Christiansen, P. Wittung-Stafshede, *FEBS Lett.* **2014**, *588*, 811.
[25] M. Senske, L. Tork, B. Born, M. Havenith, C. Herrmann, S. Ebbinghaus, *J. Am. Chem. Soc.* **2014**, *136*, 9036.
[26] P. Dubey, P. K. Chowdhury, S. Ghosh, *Biochim. Biophys. Acta (BBA) - Proteins Proteomics* **2019**, *1867*, 416.
[27] S. Tsukawaki, T. Murakami, K. Suzuki, Y. Nakazawa, *Biomed. Mater.* **2016**, *11*, 065010.
[28] K. Lundmark, G. T. Westermark, A. Olsen, P. Westermark, *Proc. Natl. Acad. Sci. U. S. A.* **2005**, *102*, 6098.
[29] J. Seo, W. Hoffmann, S. Warnke, X. Huang, S. Gewinner, W. Schollkopf, M. T. Bowers, G. von Helden, K. Pagel, *Nat. Chem.* **2017**, *9*, 39.
[30] R. I. Kunz, R. M. Brancalhao, L. F. Ribeiro, M. R. Natali, *BioMed. Res. Int.* **2016**, *2016*, 1.
[31] M. Stefani, C. M. Dobson, *J. Mol. Med.* **2003**, *81*, 678.
[32] Q. Ma, J. B. Fan, Z. Zhou, B. R. Zhou, S. R. Meng, J. Y. Hu, J. Chen, Y. Liang, *PLoS One* **2012**, *7*, 36288.
[33] R. J. Ellis, *Molecular Aspects of the Stress Response: Chaperones, Membranes and Networks*, Vol. 594, Springer, XXX **2007**, p. 1.
[34] L. A. Munishkina, E. M. Cooper, V. N. Uversky, A. L. Fink, *J. Mol. Recognit.* **2004**, *17*, 456.
[35] G. Zandomeneghi, M. R. Krebs, M. G. McCammon, M. Fandrich, *Protein Sci.* **2004**, *13*, 3314.
[36] K. Sasahara, P. McPhie, A. P. Minton, *J. Mol. Biol.* **2003**, *326*, 1227.
[37] V. Nolan, P. D. Clop, M. I. Burgos, M. A. Perillo, *Biochem. Biophys. Res. Commun.* **2019**, *515*, 190.
[38] L. A. Munishkina, A. Ahmad, A. L. Fink, V. N. Uversky, *Biochemistry* **2008**, *47*, 8993.
[39] T. Niwa, R. Sugimoto, L. Watanabe, S. Nakamura, T. Ueda, H. Taguchi, *Front. Microbiol.* **2015**, *6*, 1113.
[40] M. Assuncao, C. W. Wong, J. J. Richardson, R. Tsang, S. Beyer, M. Raghunath, A. Blocki, *Mater. Sci. Eng., C* **2020**, *106*, 110280.
[41] S. Mittal, L. R. Singh, *J. Biochem.* **2014**, *156*, 273.
[42] L. Breydo, K. D. Reddy, A. Piai, I. C. Felli, R. Pierattelli, V. N. Uversky, *Biochim. Biophys. Acta* **2014**, *1844*, 346.
[43] J. Balbo, P. Mereghetti, D. P. Herten, R. C. Wade, *Biophys. J.* **2013**, *104*, 1576.
[44] S. Palit, L. He, W. A. Hamilton, A. Yethiraj, A. Yethiraj, *J. Chem. Phys.* **2017**, *147*, 114902.
[45] F. C. Zegarra, D. Homouz, A. G. Gasic, L. Babel, M. Kovermann, P. Wittung-Stafshede, M. S. Cheung, *J. Phys. Chem. B* **2019**, *123*, 3607.
[46] S. Shahid, I. Hasan, F. Ahmad, M. I. Hassan, A. Islam, *Biomolecules* **2019**, *9*, 477.
[47] L. Lemetti, S. P. Hirvonen, D. Fedorov, P. Batys, M. Sammalkorpi, H. Tenhu, M. B. Linder, A. S. Aranko, *Eur. Polym. J.* **2019**, *112*, 539.
[48] M. S. Zafar, D. J. Belton, B. Hanby, D. L. Kaplan, C. C. Perry, *Biomacromolecules* **2015**, *16*, 606.
[49] J. Magoshi, Y. Magoshi, S. Nakamura, *Acs Symp. Ser.* **1994**, *544*, 292.
[50] T. Asakura, R. Sugino, J. M. Yao, H. Takashima, R. Kishore, *Biochemistry* **2002**, *41*, 4415.
[51] P. T. Lansbury Jr, P. R. Costa, J. M. Griffiths, E. J. Simon, M. Auger, K. J. Halverson, D. A. Kocisko, Z. S. Hendsch, T. T. Ashburn, R. G. Spencer, *Nat. Struct. Mol. Biol.* **1995**, *2*, 990.
[52] D. Li, M. M. Jacobsen, N. Gyune Rim, D. Backman, D. L. Kaplan, J. Y. Wong, *Biofabrication* **2017**, *9*, 025025.
[53] M. Lindgren, K. Sorgjerd, P. Hammarstrom, *Biophys. J.* **2005**, *88*, 4200.
[54] V. N. Uversky, J. Li, A. L. Fink, *J. Biol. Chem.* **2001**, *276*, 10737.
[55] E. S. Gil, D. J. Frankowski, S. M. Hudson, R. J. Spontak, *Mater. Sci. Eng., C* **2007**, *27*, 426.